Environmental
Science
Nano

Impact of Surface Adsorbed Biologically and Environmentally Relevant Coatings on TiO2 Nanoparticle Reactivity

SCHOLARONE™
Manuscripts

Surface coatings are crucial to understanding and predicting the photoreactivity of TiO_2 nanoparticles to form reactive oxygen species (ROS) in the environment. Herein we investigate the details and effects of environmentally and biologically relevant surface coatings on the photoreactivity of TiO_2. Our results show that protein adsorption can significantly inhibits the generation of ROS. In contrast, natural organic matter partially inhibits ROS. These results extend the understanding of mechanisms at molecular level of how macromolecules impact the photocatalytic properties of TiO_2 NPs and potential toxicity of TiO_2 NPs in environment and biological systems.

Impact of Surface Adsorbed Biologically and Environmentally Relevant Coatings on TiO₂ Nanoparticle Reactivity

Haibin Wu,[1] Liubin Huang,[1] Amber Rose,[1] Vicki H. Grassian[1,2]*

[1]Department of Chemistry & Biochemistry, University of California San Diego, La Jolla, CA 92093, United States

[2]Department of Nanoengineering, University of California San Diego, La Jolla, CA 92093, United States, Scripps Institution of Oceanography, University of California San Diego, La Jolla, CA 92093, United States

*To whom correspondence should be addressed: vhgrassian@ucsd.edu

Abstract. Studies have shown that environmentally and biologically relevant coatings on nanoparticle (NP) surfaces can significantly alter the physicochemical properties (e.g. dissolution and aggregation) of particles yet there remain some questions on how these coatings impact reactivity. In this study, we investigated molecular-level details of surface adsorption and surface reactivity of titanium dioxide (TiO₂) NPs using *in-situ* Attenuated Total Reflectance–Fourier Transform Infrared spectroscopy (ATR–FTIR) in the presence of bovine serum albumin (BSA) protein and fulvic acid (FA), which were selected as representative biologically and environmentally relevant molecules. Our results show that both BSA and FA adsorb strongly and irreversibly onto TiO₂ NP surfaces at neutral pH and these surface coatings impact the photochemical behavior of TiO₂. In particular, we show large differences in the formation of reactive oxygen species (ROS) for coated compared to uncoated TiO₂ NPs, as well as differences between the two different coatings.

In the absence of any coatings, the photooxidation of solution phase sodium benzoate (BA) to hydroxyl benzoate (major product) is observed. However, this reaction is completely inhibited when TiO_2 is coated with BSA and partially inhibited when TiO_2 is coated with FA. Additionally, we found that BSA can strongly scavenge ROS generated upon irradiation by quenching the formation of electron-hole pairs. In contrast, the behavior of FA shows photoinduced hydrophilicity of the TiO_2 coated surface and the generation of ROS, although less than that of the uncoated TiO_2 NPs. Overall, these results show that the formation of ROS from TiO_2 NPs coated by BSA and FA is reduced. Overall, this study provides insights into the impacts of environmentally and biologically relevant coatings and how they may modify the reactivity of the NPs in the environment. Furthoremore, the implications of this study extend to understanding the potential reduced toxicity and impacts of TiO_2 NPs with coatings in natural and human-impacted ecosystems.

Introduction

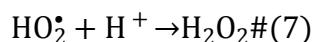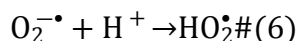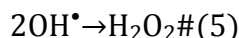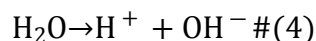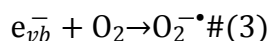Due to the abundant use of nanoparticles (NPs) utilized in industry, large quantities can end up being released into the environment as a pollutant.[1] Metal oxide NPs have been used in consumer products on a large scale. Previous research has indicated that released metal oxide NPs may exhibit some toxicity.[2, 3] With the increased use of metal oxide NPs, concerns about the safety and toxicity of nanomaterials have arisen. Titanium dioxide (TiO_2) NPs are one of the most widely used in consumer products[4] due to their unique properties,[5, 6] high biocompatibility, and high abundance.[7-10] Yet, there remains questions about the potential harm of TiO_2 NPs to both the environment and to biological organisms. As such, there has been much interest in the fate and reactivity of TiO_2 NPs.[11-14]

As a chemically stable material, the toxicity of TiO$_2$ NPs is primarily caused by reactive oxygen species (ROS) generated at the surface by photochemical processes.[11, 15] However, the reactivity of TiO$_2$ NPs can be altered in the presence of surface coatings.[16-19] For TiO$_2$ NPs released in the environment, these NPs can undergo different surface transformation processes such as adsorption, desorption and displacement.[20, 21] For example, the adsorption of natural organic matter (NOM) onto released TiO$_2$ NPs can impact their physicochemical properties including agglomeration, stability and mobility.[22-27] Fulvic acid (FA) is a representative molecule for NOM due to its high solubility at all pH values and its wide distribution in soil, sediments, and water in the environment.[28-30] FA represents a family of natural compounds derived from the decomposition of plants and animals. Previous studies have shown that the interaction of FA with nanomaterial surfaces can involve strong chemical bonds, Van der Waals interactions and/or electrostatic interactions, depending on the nature of the surface, solution phase pH and ionic strength.[31] Among the different interaction mechanisms by which NOM adsorbs onto NP surfaces, the dominant interaction is surface ligand exchange between the NP surface and functional groups on the surface which can result in irreversible adsorption, leaving a strongly adsorbed coating on the surface.[32] In addition to NOM coatings, biologically relevant molecules found in the environment can also adsorb onto NP surfaces. These biological molecules include proteins and peptides.[21, 33, 34] Among the numerous types of proteins, bovine serum albumin (BSA) is used as a model protein for serum albumin.[35] Adsorbed proteins can impact the properties of NPs (including aggregation, dissolution, reactivity and toxicity).[36] Thus, it is clear the role that surface coatings of environmentally and biologically relevant ligands play are key to understanding NPs in the environment. [37-39]

The reactivity of TiO_2 NPs involves the generation ROS including hydroxyl radical

$(OH^\bullet)$, superoxide $(O_2^{\bullet-})$, and hydrogen peroxide (H_2O_2).[40] Different reactions to form these

species are represented in Reactions 1-8 below:

$$TiO_2 + h\nu \rightarrow h_{vb}^+ + e_{vb}^- \#(1)$$

$$h_{vb}^+ + H_2O \rightarrow OH^\bullet + H^+ \#(2)$$

$$e_{vb}^- + O_2 \rightarrow O_2^{-\bullet} \#(3)$$

$$H_2O \rightarrow H^+ + OH^- \#(4)$$

$$2OH^\bullet \rightarrow H_2O_2 \#(5)$$

$$O_2^{-\bullet} + H^+ \rightarrow HO_2^\bullet \#(6)$$

$$HO_2^\bullet + H^+ \rightarrow H_2O_2 \#(7)$$

$$H_2O_2 + e_{vb}^- \rightarrow OH^\bullet + OH^- \#(8)$$
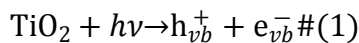
TiO_2 NPs first form e^-/h^+ pairs, i.e. the formation of a hole and an electron excited by a

photon with an energy greater than that of the bandgap (1). With a formation of a hole,

water can be oxidized to hydroxyl radicals (2). Hydroxyl radicals can then interact to form

hydrogen peroxide (5). Through a series of steps (3, 4 and 6), oxygen in the system is

reduced to superoxide which can then react with protons, resulting in the generation of

hydrogen peroxide (7). Additionally, hydrogen peroxide can be reduced to a hydroxyl

radical and hydroxide ion (8).

In aqueous systems, even though direct oxidation still occurs on the surface, ROS

are primarily responsible for the photocatalytic properties of TiO_2 NPs in different

applications, including dye degradation.[41-46] These same reactions can also cause phototoxcity to organisms in the enviroment.[11, 12, 47, 48] How surface coatings play a crucial role in the formation of ROS is important to understand. A previous study by Long *et al.* suggests that NOM coatings such as humic acid (HA) on TiO_2 NPs can serve as scavengers to quench holes, consequently weakening the capability of these NPs for photochemical degradation of phenol.[49] In addition, a study focused on the denaturation of adsorbed proteins indicates that, to some degree, the protein corona prevents phototoxicity.[33, 50] However, these studies have not been able to reveal detailed, molecular-based mechanisms that occur on the surface.

Bürgi and co-workers have studied photocatalysis of TiO_2 using *in-situ* ATR–FTIR methods, focusing on the photochemical processes involving organic acids, such as oxalic and malonic acids.[51-53] Their findings provide important insights into how adsorbed ligands affect the photocatalytic performance of TiO_2. Although the adsorption of ligands on nanomaterials has been extensively studied by ATR–FTIR spectroscopy,[20, 54-58] there are few reports about the mechanisms and roles of environmentally and biologically relevant coatings in reactions and their impact on the photoactivity of TiO_2 NPs in the environment. Therefore, in this study we have used two model macromolecules, BSA and FA, that represent biologically and environmentally relevant molecules. The findings of this work provide insights about how NPs behave in the environment and the change in potential toxicity. Herein, we employed the use of mass spectrometry and ATR–FTIR spectroscopy to further explore photochemical reactions. ATR–FTIR spectroscopy is a technique that allows for *in-situ* monitoring of adsorbed species and chemical processes by measuring changes in the vibrational spectra.

Experimental Methods

Materials. TiO$_2$ NPs were purchased from Aldrich (vendor reported size 21nm, $\geq$99.5%). Solutions of sodium benzoate (BA, $\geq$99.5%, Sigma-Aldrich), Suwannee River fulvic acid (FA, International Humic Substances Society, Minneapolis, MN) and bovine serum albumin (BSA, $\geq$ 98%, Sigma-Aldrich) were prepared at pH 7 for all experiments. Sodium hydroxide (NaOH, 1N; Fisher Scientific) and hydrochloric acid (HCl, 1N; Fisher Scientific) were used to adjust pH. All the solutions were prepared with Milli-Q water.

ATR–FTIR spectroscopy. ATR–FTIR measurements were made following well-established protocols from previous studies with some modifications for photochemical reactions.[20, 21, 56] ATR–FTIR spectra were produced by using a 500 μL horizontal ATR flow cell with an AMTIR window (Pike Technologies Inc.) in a Nicolet iS 10 FTIR Spectrometer equipped with an MCT–A detector. Spectra were collected with 264 scans at 4 cm^{-1} resolution in the AMTIR window range (4000 – 750 cm^{-1}). The TiO$_2$ NP thin film was prepared by drying 1 mL of 1g L^{-1} TiO$_2$ in Milli–Q water on the AMTIR crystal in a dry air flow overnight. A water flow (pH 7) over the TiO$_2$ NP film was introduced for at least 30 min to remove any loose particles on the film prior to collecting the background. For adsorption, 0.5 g L^{-1} BSA, and 0.1 g L^{-1} fulvic acid solutions were used to fully cover the TiO$_2$ NP surface. The solution of BSA or FA was flowed over the TiO$_2$ NP film for 2 hrs at a fixed flow rate (~0.4 mL min^{-1}) to cover the TiO$_2$ surface. Absorption spectra were collected at 5 minute intervals. The photochemical studies of BSA and FA on TiO$_2$ NPs followed similar experimental protocols in that BSA or FA solution was introduced into the aqueous phase over the TiO$_2$ NP film prior to light exposure. After flowing water solutions containing BSA or FA for 2 hrs, surface adsorption reached an equillbrium as

measured by the integrated absorbances of the absorption bands as a function of time. The flow was halted and then a solar simulator (An LCS–100 solar simulator, model 94011A, Oriel, Newport, equipped with an AM1.5G filter and water filter) was used for *in situ* irradiation of the TiO_2 nanoparticles through a quartz window. An unncoated TiO_2 NP film was also studied, as a control, following similar procedures as described above, but using water instead of BSA or FA solutions. The ATR-FTIR spectra were collected every 5 min for 2 hrs. To test for the formation of hydroxyl radicals and subsequent reaction with BA on uncoated and coated TiO_2 nanoparticles, the experiments followed three sequential steps: (1) adsorption of BSA or FA; (2) introduction of BA , 10 mM BA solution was introduced into the ATR flow cell with the TiO_2 NP film for two hours to equilibrate in the dark prior to exposure to light; (3) exposure to broadband irradiation. Spectra were collected at an interval of every 5 minutes.

Batch reactor photochemical experiments. TiO_2 NPs were first mixed with 0.1 mg ml^{-1} FA or 0.5 mg ml^{-1} BSA solution to coat the surface with a loading amount of 2 g L^{-1} for 12 hrs. The coated TiO_2 NPs were then separated from the suspension by centrifuging for 10 mins at 10,000 rpm. The precipitate was washed with water to remove any excess solution remaining on the surface. The samples were transferred to a vacuum desiccator to dry, then ca. 20 mg of coated TiO_2 powder was added to a 20 mL glass vial with 10 mL of 2 mM BA solution. The vial was covered with foil and transferred into a bath sonicator to sonicate for 10 mins. The well-mixed suspensions were then exposed to light generated by a solar simulator with vigorous stirring for 6 hrs. After reaction, the suspensions were transferred to 15 mL centrifuge tubes and centrifuged for 10 mins at 10,000 rpm. The resulting

supernatant was filtered through an MCE membrane (Millex–GS, 0.22 um) and kept

refrigerated for further mass spectrometric analysis.

Mass spectrometry analyses of photooxidation products. The supernatant collected from

the batch reactor was analyzed by a high-resolution hybrid linear ion trap mass

spectrometer equipped with a heated electrospray ionization source (HESI–HRMS,

Thermo Orbitrap Elite) using direct infusion mode. Prior to experiments, the samples were

diluted by a factor of 10 with acetonitrile. Data were collected in negative ionization mode

over the mass range of 50–2000 Da, with the spray voltage set at 2.60 kV, capillary

temperature at 325 ℃ and S-lens at 60%.

Results and Discussion

ATR–FTIR spectroscopy of BSA and FA adsorption on TiO$_2$ NPs. ATR–FTIR spectroscopy

was employed to study ligand adsorption, photochemical reactions of ligands on TiO$_2$ NPs,

as well as photochemical oxidation of BA on TiO$_2$ NPs with coatings at pH 7. ATR–FTIR

spectra were recorded as a function of time in the presence of BSA (Figure 1a) and FA

(Figure 1b) on a TiO$_2$ surface. These spectra were referenced to a water-TiO$_2$ film at the

same pH. There is an increase in intensity of several peaks in the spectral range extending

from 900 to 2000 cm^{-1}, as a function of time. Peak assignments for BSA and FA have been

made previously and are listed in Table 1. For the adsorbed BSA spectra (Figure 1a), the

amide I band appears at 1651 cm^{-1}.[59] The N–H bending and C–N stretching of the amide

II band appears at a vibrational frequency around 1545 cm^{-1}. The other two absorption

features at 1453 and 1400 cm^{-1} are due to C–H bending and the amide III band, respectively.

For FA adsorption, there are multiple functional groups of FA involved in the interaction

with TiO$_2$ including: carbonyls, amides, carboxylates, phenols, polysaccharides, and

alcohol hydroxyls.[20, 60] In the adsorbed FA spectra (Figure 1b), the dominant absorption

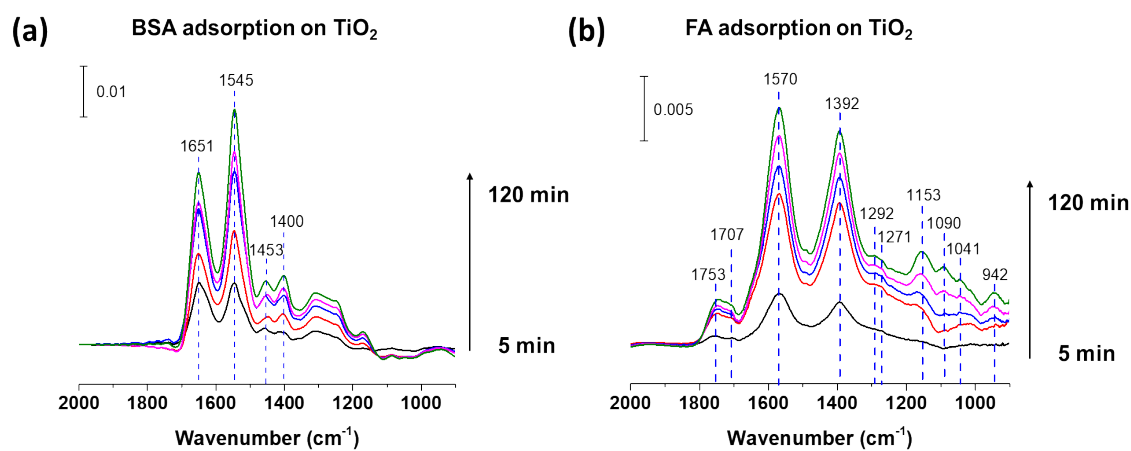bands correspond to the asymmetric and symmetric carboxylate vibrations appearing at

Figure 1. ATR–FTIR spectra of the molecular adsorption on TiO$_2$ NP film, (a) 0.5 mg/ml
BSA, (b) 0.1 mg/ml FA, respectively, as a function of time. The adsorption spectra shown
were collected at 5 min (black), 30 min (red), 60 min (blue), 90 (magenta), 120 min (green).

1570 and 1392 cm^{-1}, respectively. In addition to the strong asymmetric and symmetric

vibrations of carboxylate, the absorption band at 1292 cm^{-1} is assigned to the bending of

the –COO–Ti groups.[20, 21] These vibrational bands indicate that FA primarily binds to the

TiO$_2$ NP surface via the carboxylate group. Other characteristic absorption bands include

C=O stretching at 1753 and 1707 cm^{-1}. By flowing the solution over the TiO$_2$ film for 2

hrs, the intensity of the spectra has reached a maximum, indicating the surface has been

fully covered by BSA or FA (see in Electronic Supplemental Information (ESI), Figure

S1).

Table 1. Assignment of the vibrational frequencies of BSA, FA and BA.

Biological and/or Chemical Species	Vibrational Mode	Adsorbed Species [this work (cm^{-1})]	Literature (cm^{-1}) [21, 29, 56, 61-66]	
BSA	amide I	1651	1695	1630
	amide II	1545	1550	

	δ (C-H)	1453	1500-1400
	amide III and/or υ (C-O)/ υ (C-O-C)/ υ (C-C)	1400	1400 1000
	υ (C=O)	1753,1707	1720, 1640
	$υ_{asym}$ (COO⁻)	1570	1590 1550
	δ (C-H)	1451	1450
FA	$υ_{sym}$(COO-)/OH def	1392	1350
	δ (O-C=O)	1292	1292
	υ (phenol C-OH)	1271	1270
	υ (C-C, C-O)	1153, 1090, 1041, 942	1200 1000
	υ (C=C)	1600, 1557, 1497	1660 1450
	$υ_{sym}$(COO-)/OH def	1391	1400 1391
BA	δ (C-H)	1434	1450
	δ (CO-H)	1309,1320	1320, 1338
	υ (C-OH)	1268	1297,1274, 1269,1245

ATR–FTIR spectra monitoring of photochemical processes on TiO₂ NPs. Figure 2 shows

ATR–FTIR spectra of pure water irraradiated on a TiO$_2$ NP film as a function of time. The

water bending mode can be seen at 1636 cm^{-1} and the increase of this peak suggests water

adsorption upon irradiation, indicating photoinduced superhydrophilicity of TiO$_2$ NPs.[67] It

should be noted that the region below 1200 cm^{-1} also grows with irradiation. The prominent

peaks located at 1100 and 1084 cm^{-1} are attributed to adsorbed superoxide on the surface.[68-

70] Another peak at 980 cm^{-1} is possibly due to a terminal Ti $\equiv$ O that is believed to be an

intermediate state in photocatalytic processes.[71] As reported as previous studies, it is likely

that H$_2$O$_2$, which exhibits an IR vibrational frequency around 870 cm^{-1}, forms in addition

10

to superoxide.[72, 73] However, the peak at 870 cm^{-1} possibly merged into this broader

absorption feature. Thus, TiO$_2$ has a surface that is very reactive to the generation of ROS

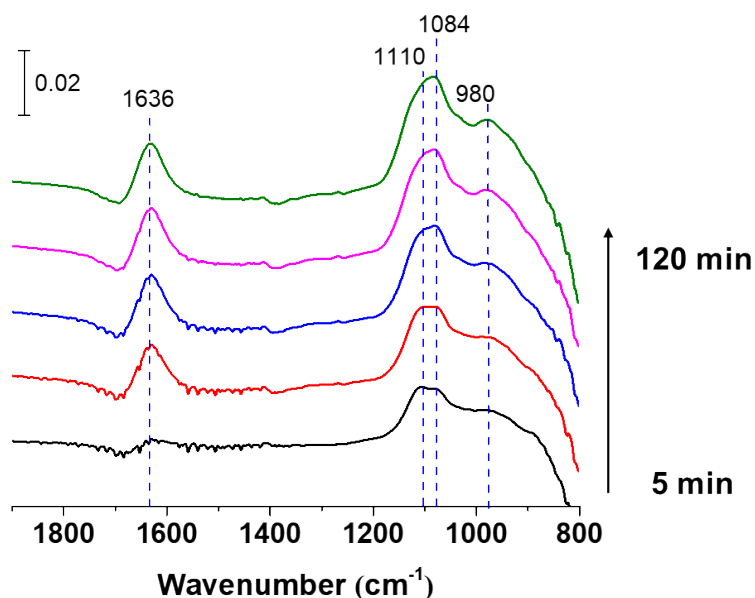in water including H$_2$O$_2$ and superoxide radicals.

Figure 2. ATR-FTIR spectra following broadband irradiation of pure water on TiO$_2$ NPs. The spectra shown were collected at 5 min (black), 30 min (red), 60 min (blue), 90 min (magenta), 120 min (green) and are referenced to an initial dark spectrum of the H$_2$O--TiO$_2$ film.

ATR–FTIR spectra monitoring of photochemical processes with coating molecules on TiO$_2$

NPs. The photocatalytic behavior of TiO$_2$ coated by BSA and FA was investigated *in-situ*

by ATR–FTIR. During this process, the corresponding solution remained above the film

when irradiated with light. No vibrational frequency shifts are seen for the major peaks of

BSA (Figure 3a). Interestingly, a new peak at 1761 cm^{-1} appears to grow at later irradiation

times. Although this peak has not been reported in previous work,[33, 34] it is likely that it

comes from the photooxidation of BSA on the TiO$_2$ surface. It is also worth noting that the

intensity of the amide I band at 1651 cm^{-1} increases significantly with irradiation time. In

previous studies, it has been suggested that this was caused by changes in secondary

11

structure upon irradiation.[33] As shown previously,[21] BSA has a strong binding affinity for

the TiO_2 surface; therefore, generated ROS or excited holes from TiO_2 may first react with

adsorbed BSA molecules. This causes spectral changes of BSA induced by irradiation. The

resulting IR spectra are shown in Figure 3. The intensity of each spectrum increased with

irradiation time due to a higher background induced by irradiation.[74, 75] Additionally, more

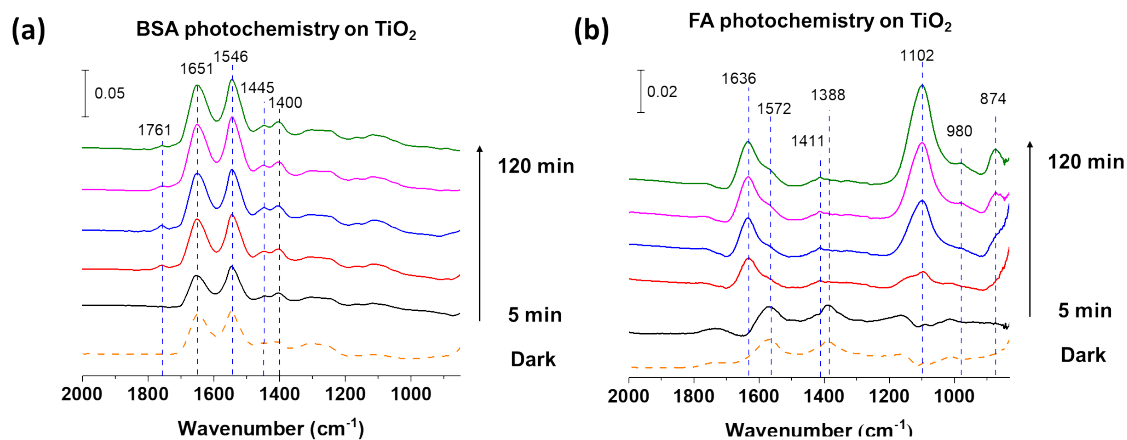BSA molecules may be adsorbed on the surface upon irradiation, resulting in an intensity

increase.

Figure 3. ATR–FTIR spectra of the photochemical process of coated TiO_2 NPs, (a) BSA-coated TiO_2, (b) FA-coated TiO_2. The spectra shown were collected at 5 min (black), 30 min (red), 60 min (blue), 90 (magenta), 120 min (green), and the dashed orange line represents a dark control.

Adsorbed FA is also able to quench the generation of trapped holes so that the

production of hydroxyl radicals is inhibited but to a much lesser extent.[30, 37, 76, 77] In addition,

the displacement between FA and surface hydroxyl group upon FA adsorption on TiO_2

surfaces can also reduce the amount of surface hydroxyl groups which will then reduce the

amount of hydroxyl radicals formed. In contrast to BSA-coated TiO_2 NPs, the spectra of

adsorbed FA upon irradiation changes with time (Figure 3b). The first spectrum, collected

at t = 5 min after irradiation, shows characteristic vibrations of adsorbed FA on TiO_2 NPs

12

which include the asymmetric and symmetric vibrations of COO⁻ groups at 1572 and 1388 cm⁻¹, respectively. As irradiation time increases, the symmetric peak shifts to 1411 cm⁻¹ after 30 min, while the asymmetric peak does not change vibrational frequency but instead merges with a peak at 1636 cm⁻¹ (adsorbed water on the TiO_2 surface). Bürgi et al. proposed that directly bonded organic molecules can be oxidized by excited holes and the newly oxidized species would then bind to the surface through other binding modes.[51, 53] Therefore, it is plausible that these FA can change their binding modes upon irradiation due to TiO_2 surface changes[78] and photodegradation.[79, 80] This process may decrease the FA surface coverage, which leads to more water molecules adsorbed to the surface leading to, as shown in Reaction 4, oxidation of adsorbed water as a source of ROS. It is worth noting that three new peaks in the low vibrational frequency range below 1200 cm⁻¹ (1102, 980, and 874 cm⁻¹) are likely from surface ROS intermediates generated by irradiation. The peak at 874 cm⁻¹ is assigned to hydrogen peroxide (reported IR frequency for hydrogen peroxide is 877 cm⁻¹).[73] The other two peaks at 1102 and 980 cm⁻¹ are possibly from an adsorbed superoxide intermediate with Ti^{4+} and $Ti \equiv O$, respectively.[70, 71] Therefore, these peaks provide aevidence for the formation of ROS on the FA-coated TiO_2 surface. FA also has a high degree of conjugation in its structure with the presence of aromatics and olefinic groups. This can enable an electron transfer pathway, which helps to enhance oxygen reduction.[81] The photoinduced surface change affects the binding mode of FA on the TiO_2 surface and can give rise to surface regions whereby water can adsorb on the surface. This can be seen in the IR spectra, where photoinduced water adsorption and oxygen reduction products such as superoxide and hydrogen peroxide were observed. A large amount of ROS are generated with irradiation time, therefore, adsorbed FA can be rapidly oxidized

13

making it more difficult to observe any increase in peak intensities due to enhanced

adsorption as found for BSA.

ATR–FTIR spectra monitoring of photochemical oxidation of BA on TiO$_2$ NPs. Hydroxyl

groups are hard to detect in solution and here we used BA as a probe molecule, since BA

can react with hydroxyl radicals to produce a series of product compounds. BA in solution

was introduced into the ATR cell over coated and uncoated TiO$_2$ films in the dark. The

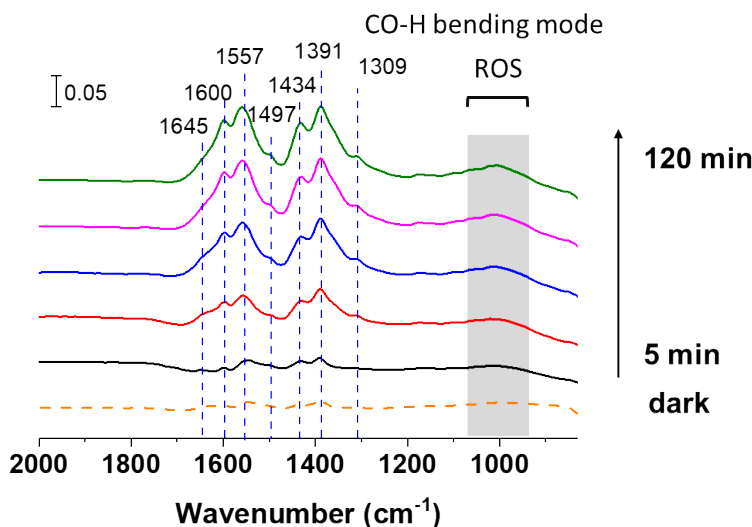photochemical   reaction   for   BA   solution   on   bare   TiO$_2$ NPs

Figure 4. ATR-FTIR spectra of the photochemical process of 10 mM BA on TiO$_2$ NPs. The spectra shown were collected at initial spectrum in the dark (black), 5 min (red), 30 min (blue), 60 min (magenta), 90 min (green), 120 min (orange), and the dashed orange line represents a dark control.

was first investigated and the spectra are shown in Figure 4. The first spectrum was

collected without light irradiation (initial solution). The characteristic peaks of BA are

located in the region from 1600 to 1391 cm^{-1}: they are primarily from the symmetric

stretching vibration of carboxylate (1391 cm^{-1}), bending of C–H (1434 cm^{-1}) and the

breathing modes of the benzene ring (1600, 1557, and 1497 cm^{-1}).[65] The asymmetric

stretching of carboxylate likely overlaps with these peaks. The peak at 1645 cm^{-1} is attributed to the bending mode of adsorbed water on the TiO$_2$ surface. As seen in Figure 4, the intensity of the peaks increases with irradiation time. It is interesting that a new shoulder peak at 1309 cm^{-1} appears after irradiation, which is close to the bending mode of CO–H in   hydroxyl   benzoate.[66,]   [82]
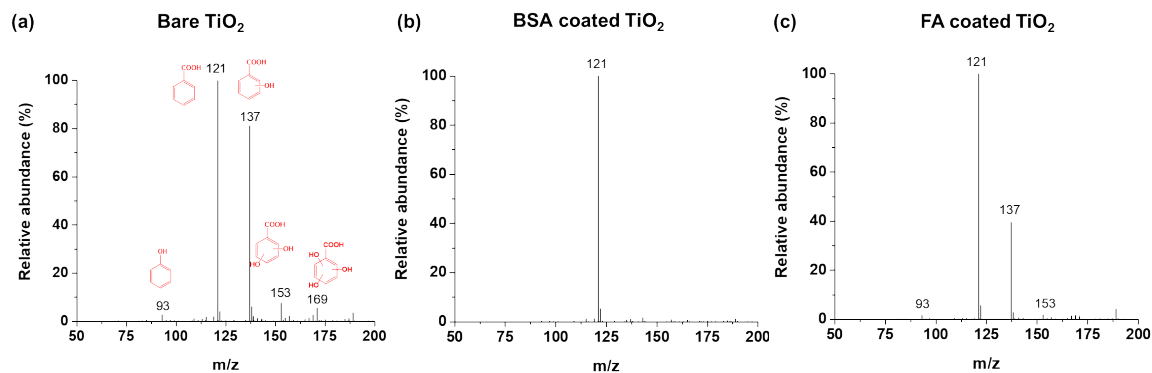

Figure 5. Mass spectra of benzoate reacted with (a) bare TiO$_2$, (b) BSA-coated TiO$_2$ and (c) FA-coated TiO$_2$.

In addition, a broad peak from ROS (i.e adsorbed superoxide and hydrogen peroxide) arises with irradiation time, indicating the formation of ROS on the BA-covered surface. This suggests that BA on bare TiO$_2$ may oxidized to hydroxyl benzoate. In order to confirm this, mass spectrometry was used. Figure 5a shows the mass spectrum of benzoic acid when reacted with bare TiO$_2$ NPs under irradiation conditions. A pronounced peak at *m/z* 137, with the formula of C$_7$H$_5$O$_3$$^-$, dominates the spectrum. Additionally, m/z 93 (C$_6$H$_5$O$^-$), 153 (C$_7$H$_5$O$_4$$^-$), and 169 (C$_7H_5O_5$$^-$) are also observed. Figure 6 displays a possible mechanism for the formation of these products. It is well known that ROS, such as hydroxyl radical, can be generated on the TiO$_2$ surface under UV conditions.[40] Therefore, the formation of these products arise from the oxidation of BA by hydroxyl radicals. The reaction of BA with hydroxyl radicals is initiated via an electron transfer step that generates a

carboxyphenyl radical intermediate. This radical can react with H_2O to form hydroxyl benzoic acid (m/z 137) or undergo decarboxylation to produce a phenyl radical resulting in the formation of phenol (m/z 93). Upon further oxidation, the carboxyphenyl radical intermediate can also be converted to dihydroxy (m/z 153) and trihydroxy benzoic acid (m/z 169), in addition to other products.
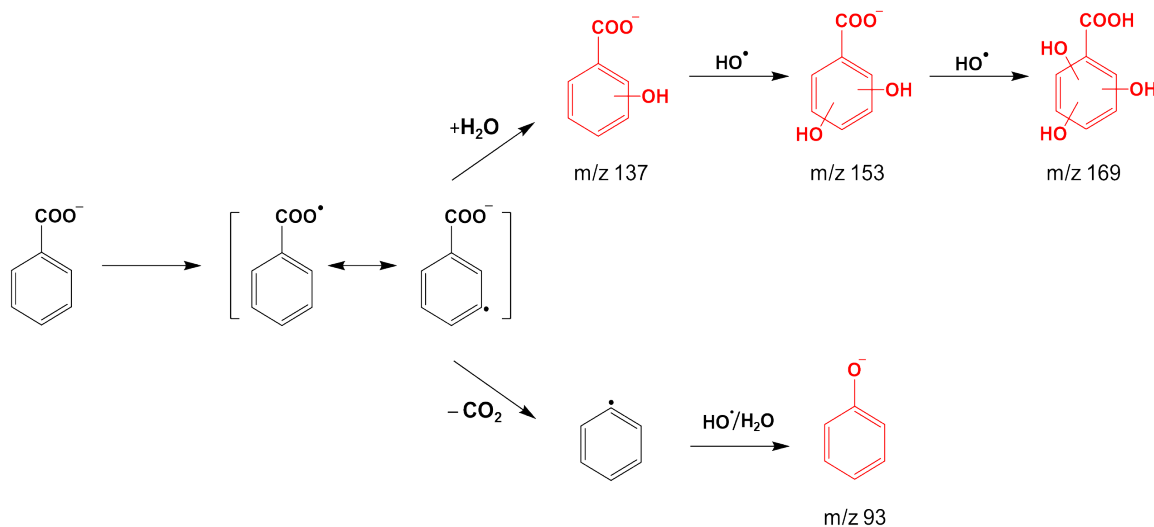

Figure 6. A proposed pathway of BA oxidation.

In order to understand the effects of coating molecules on photochemical processes in the presence of BA, BA solutions were first introduced onto BSA- or FA-coated NP films in the dark. The ATR—FTIR dark spectra are provided ESI, Figure S2), i.e. adsorption of BA on pre-coated NPs. All spectra preserve the initial IR characteristic absorptions. It is clear that there are no observed peak shifts due to displacement reactions by BA. Therefore, these data suggest that BA in this process interacts with the surface coatings and not directly with the TiO_2 surface. Benzoic acid has been reported to interact with tryptophan residues in BSA via van der Waals forces and electrostatic interactions with the positively charged amino acid.[83, 84] Compared to BSA-only coated spectra, the

peak at 1761 cm^{-1} is weaker in the presence of BA (Figure 7a). Additionally, a peak at 1100

cm^{-1} is seen following irradiation which may be due to oxidation of BSA in the presence

of BA.

Overall, the BSA coating strongly inhibits the oxidation of BA by hydroxyl radicals.

When the FA-coated surface was exposed to the BA solution, the first spectrum closely

resembles that of the FA-only coated surface spectra (Figure 7b), which suggests again that

BA has little interaction with the TiO$_2$ surface. The possible surface ROS intermediates

generated by irradiation appear in the same range as previously shown for the FA-coated

surface in the absence of BA. There are, however, some small spectral differences from the

presence of BA. A new peak at 1268 cm^{-1} is observed in the spectra, which is possibly

from the C–OH stretching mode in hydroxybenzoic acid.[66] These new peaks suggest that

BA is oxidized to hydroxyl benzoate on the FA-coated surface.
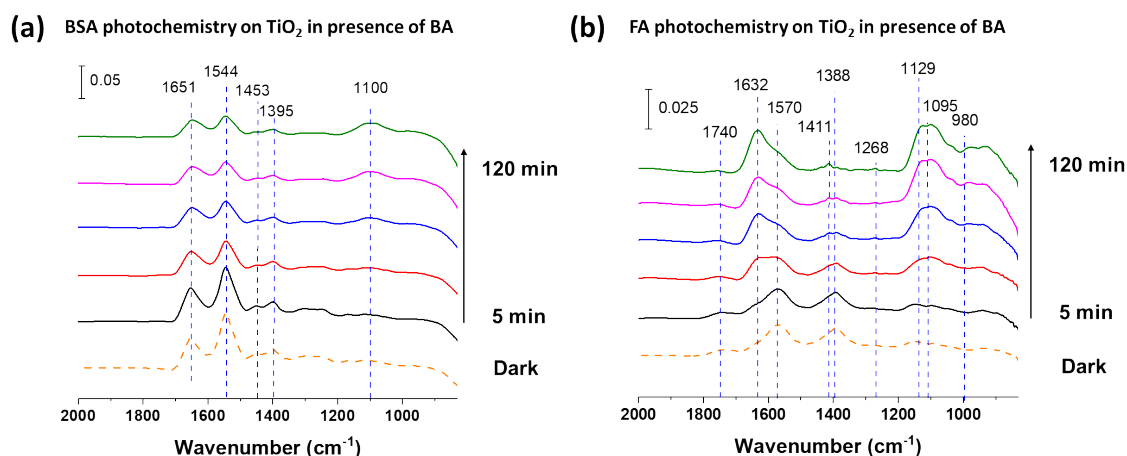
Figure 7. ATR-FTIR spectra of photochemical process of coated TiO$_2$ NPs in presence of 2 mM BA, (a) BSA coated TiO$_2$, (b) FA coated TiO$_2$. The spectra shown were collected at 5 min (black), 30 min (red), 60 min (blue), 90 (magenta), 120 min (green), and the dashed orange line represents a dark control.

The mass spectral data further corroborate the results shown with ATR-FTIR spectroscopy discussed above. As shown in Figure 5b, there is only one pronounced peak for BA at *m/z* 121 on the BSA-coated surface. However, m/z 93 ($C_6H_5O^-$) and 153 ($C_7H_5O_4^-$) are also observed on the FA-coated surface (Figure 5c) in addition to the dominant peak at *m/z* 137 for hydroxy benzoate. The products for FA-coated TiO_2 are less than that of bare TiO_2, indicating that FA prohibits hydroxyl radical production. Moreover, these peaks disappear in the reaction of BA with BSA-coated TiO_2, suggesting that BSA has a much stronger inhibition effect on the production of hydroxyl radicals than FA.

Conclusions

BSA and FA, as representative ligands of biological and environmental significance, were chosen to study their effects on the generation of ROS under irradiation of TiO_2 nanoparticles through *in-situ* ATR–FTIR and mass spectrometry. The photochemical IR measurements demonstrate formation of ROS on bare TiO_2 NP surfaces. However, as the surface is coated with biological molecules (i.e. BSA), ROS generation (e.g. superoxide and hydrogen peroxide) is strongly inhibited. Instead, BSA is a scavenger, showing a new spectral feature which indicates BSA oxidation. In contrast to BSA, FA-coated TiO_2 NP surfaces show more reactivity in generating ROS. Based on our study, the interaction between coating molecules and surfaces of nanomaterials shows significant impacts on the generation of ROS and holes, which are highly relevant to the reactivity of TiO_2 NPs. FA can change binding modes, allowing for the adsorption of water molecules, resulting in only partial inhibition of ROS. Upon further study of detection of hydroxyl radicals by BA, BA does not show signs of oxidation on BSA-coated surfaces, but it is oxidized on FA-coated surfaces upon irradiation. In addition to the *in-situ* spectroscopic

measurements, mass spectrometry was also utilized to analyze the products on three surfaces (bare, BSA-coated and FA-coated). These results indicate that the presence of BA alters the interaction of BSA with TiO_2 surfaces, thus prohibiting oxidation of BA by hydroxyl radicals. Therefore, the ability for ROS generation on TiO_2 NPs with different coatings follows this sequence: bare TiO_2 > FA–TiO_2 > BSA–TiO_2. As indicated by the results in this work, the reactivity in generating ROS from TiO_2 NPs released to the environment or biological systems can be largely reduced or restricted by adsorbing macromolecules such as proteins and NOM. Thus, TiO_2 coated with macromolecules in organisms and natural waters will be potentially less toxic than models have predicted, since this releases less ROS compared to bare TiO_2. Therefore, this study shows the importance of biological and environmental ligands on modulating the reactivity of TiO_2 nanoparticles in the environment.

Conflicts of interest

There are no conflicts to declare.

Acknowledgements

References

1.   K. L. Garner, S. Suh and A. A. Keller, Assessing the risk of engineered nanomaterials in the environment: development and application of the nanofate model, *Environ. Sci. Technol*, 2017, **51**, 5541-5551.

2.   A. Wongrakpanich, I. A. Mudunkotuwa, S. M. Geary, A. S. Morris, K. A. Mapuskar, D. R. Spitz, V. H. Grassian and A. K. Salem, Size-dependent cytotoxicity of copper oxide nanoparticles in lung epithelial cells, *Environ. Sci. Nano*, 2016, **3**, 365-374.

3.   T. J. Brunner, P. Wick, P. Manser, P. Spohn, R. N. Grass, L. K. Limbach, A. Bruinink and W. J. Stark, In vitro cytotoxicity of oxide nanoparticles: comparison to asbestos, silica, and the effect of particle solubility, *Environ. Sci. Technol*, 2006, **40**, 4374-4381.

4.   T. G. Smijs and S. Pavel, Titanium dioxide and zinc oxide nanoparticles in sunscreens: focus on their safety and effectiveness, *Nanotechnol. Sci. Appl.*, 2011, **4**, 95-112.

5.   R. Daghrir, P. Drogui and D. Robert, Modified TiO_2 for environmental photocatalytic applications: a review, *Ind. Eng. Chem*, 2013, **52**, 3581-3599.

6.   Y. Wang, Q. Wang, X. Zhan, F. Wang, M. Safdar and J. He, Visible light driven type II heterostructures and their enhanced photocatalysis properties: a review, *Nanoscale*, 2013, **5**, 8326-8339.

7.   Z. Li, R. Yang, M. Yu, F. Bai, C. Li and Z. L. Wang, Cellular level biocompatibility and biosafety of ZnO nanowires, *J. Phys. Chem. C*, 2008, **112**, 20114-20117.

8.   Z. Ji, X. Jin, S. George, T. Xia, H. Meng, X. Wang, E. Suarez, H. Zhang, E. M. V. Hoek, H. Godwin, A. E. Nel and J. I. Zink, Dispersion and stability optimization of TiO_2 nanoparticles in cell culture media, *Environ. Sci. Technol*, 2010, **44**, 7309-7314.

9.   M. Ramani, M. C. Mudge, R. T. Morris, Y. Zhang, S. A. Warcholek, M. N. Hurst, J. E. Riviere and R. K. DeLong, Zinc oxide nanoparticle-poly i:C RNA complexes: implication as therapeutics against experimental melanoma, *Mol Pharm*, 2017, **14**, 614-625.

10.   S. Singh, V. D'Britto, A. Bharde, M. Sastry, A. Dhawan and B. L. V. Prasad, Bacterial synthesis of photocatalytically active and biocompatible TiO_2 and ZnO nanoparticles, *International Journal of Green Nanotechnology: Physics and Chemistry*, 2010, **2**, 80-99.

11.   T. Tong, A. Shereef, J. Wu, C. T. T. Binh, J. J. Kelly, J.-F. Gaillard and K. A. Gray, Effects of material morphology on the phototoxicity of nano-TiO_2 to bacteria, *Environ. Sci. Technol*, 2013, **47**, 12486-12495.

12.   X. Zhu, J. Zhou and Z. Cai, TiO_2 nanoparticles in the marine environment: impact on the toxicity of tributyltin to abalone (haliotis diversicolor supertexta) embryos, *Environ. Sci. Technol*, 2011, **45**, 3753-3758.

13.   M. Simonin, A. Richaume, J. P. Guyonnet, A. Dubost, J. M. F. Martins and T. Pommier, Titanium dioxide nanoparticles strongly impact soil microbial function by affecting archaeal nitrifiers, *Sci. Rep.*, 2016, **6**, 33643.

14.   S. Shakiba, A. Hakimian, L. R. Barco and S. M. Louie, Dynamic intermolecular interactions control adsorption from mixtures of natural organic matter and protein onto titanium dioxide nanoparticles, *Environ. Sci. Technol*, 2018, **52**, 14158-14168.

15.   N. Liu, Y. Chang, Y. Feng, Y. Cheng, X. Sun, H. Jian, Y. Feng, X. Li and H. Zhang, {101}−{001} surface heterojunction-enhanced antibacterial activity of titanium dioxide nanocrystals under sunlight irradiation, *ACS Appl. Mater. Interfaces*, 2017, **9**, 5907-5915.

16.   Z. Zhou, J. Son, B. Harper, Z. Zhou and S. Harper, Influence of surface chemical properties on the toxicity of engineered zinc oxide nanoparticles to embryonic zebrafish, *Beilstein J. Nanotechnol.*, 2015, **6**, 1568-1579.

17.   A. Praetorius, M. Scheringer and K. Hungerbühler, Development of environmental fate models for engineered nanoparticles—a case study of TiO_2 nanoparticles in the rhine river, *Environ. Sci. Technol*, 2012, **46**, 6705-6713.

18.   J. Labille, J. Feng, C. Botta, D. Borschneck, M. Sammut, M. Cabie, M. Auffan, J. Rose and J.-Y. Bottero, Aging of TiO_2 nanocomposites used in sunscreen. Dispersion and fate of the degradation products in aqueous environment, *Environ. Pollut.*, 2010, **158**, 3482-3489.

19.   B. van Ravenzwaay, R. Landsiedel, E. Fabian, S. Burkhardt, V. Strauss and L. Ma-Hock, Comparing fate and effects of three particles of different surface properties: nano-TiO_2, pigmentary TiO_2 and quartz, *Toxicol. Lett.*, 2009, **186**, 152-159.

20.   S. Jayalath, H. Wu, S. C. Larsen and V. H. Grassian, Surface adsorption of suwannee river humic acid on TiO_2 nanoparticles: a study of pH and particle size, *Langmuir*, 2018, **34**, 3136-3145.

21.   H. Wu, N. I. Gonzalez-Pech and V. H. Grassian, Displacement reactions between environmentally and biologically relevant ligands on TiO_2 nanoparticles: insights into the aging of nanoparticles in the environment, *Environ. Sci. Nano*, 2019, **6**, 489-504.

22.   J. A. Gallego-Urrea, J. Perez Holmberg and M. Hassellöv, Influence of different types of natural organic matter on titania nanoparticle stability: effects of counter ion concentration and pH, *Environ. Sci. Nano*, 2014, **1**, 181-189.

23.   F. Loosli, P. Le Coustumer and S. Stoll, Effect of natural organic matter on the disagglomeration of manufactured TiO_2 nanoparticles, *Environ. Sci. Nano*, 2014, **1**, 154-160.

24.   R. F. Domingos, N. Tufenkji and K. J. Wilkinson, Aggregation of titanium dioxide nanoparticles: role of a fulvic acid, *Environ. Sci. Technol*, 2009, **43**, 1282-1286.

25.   R. F. Domingos, Z. Rafiei, C. E. Monteiro, M. A. K. Khan and K. J. Wilkinson, Agglomeration and dissolution of zinc oxide nanoparticles: role of pH, ionic strength and fulvic acid, *Environ. Chem.*, 2013, **10**, 306-312.

26.   G. Chen, X. Liu and C. Su, Distinct effects of humic acid on transport and retention of TiO_2 rutile nanoparticles in saturated sand columns, *Environ. Sci. Technol*, 2012, **46**, 7142-7150.

27.   I. Chowdhury, D. M. Cwiertny and S. L. Walker, Combined factors influencing the aggregation and deposition of nano-TiO_2 in the presence of humic acid and bacteria, *Environ. Sci. Technol.*, 2012, **46**, 6968-6976.

28.   T. H. Yoon, S. B. Johnson and G. E. Brown, Adsorption of suwannee river fulvic acid on aluminum oxyhydroxide surfaces: an in situ ATR-FTIR study, *Langmuir*, 2004, **20**, 5655-5658.

29.   A. U. Baes and P. R. Bloom, Diffuse reflectance and transmission fourier transform infrared (DRIFT) spectroscopy of humic and fulvic acids, *Soil. Sci. Soc. Am. J.*, 1989, **53**, 695-700.

30.   W. Wu, G. Shan, Q. Xiang, Y. Zhang, S. Yi and L. Zhu, Effects of humic acids with different polarities on the photocatalytic activity of nano-TiO_2 at environment relevant concentration, *Water Res.*, 2013, **122**, 78-85.

31.   A. Philippe and G. E. Schaumann, Interactions of dissolved organic matter with natural and engineered inorganic colloids: a review, *Environ. Sci. Technol*, 2014, **48**, 8946-8962.

32.   K. Yang, D. Lin and B. Xing, Interactions of humic acid with nanosized inorganic oxides, *Langmuir*, 2009, **25**, 3571-3576.

33.   A. Bouhekka and T. Bürgi, In situ ATR-IR spectroscopy study of adsorbed protein: visible light denaturation of bovine serum albumin on TiO_2, *Appl. Surf. Sci.*, 2012, **261**, 369-374.

34.   A. Bouhekka and T. Bürgi, Photodegradation of adsorbed bovine serum albumin on TiO_2 anatase investigated by in-situ ATR-IR spectroscopy, *Acta Chim. Slov.*, 2012, **59**, 841–847.

35.   F. Nasser and I. Lynch, Secreted protein eco-corona mediates uptake and impacts of polystyrene nanoparticles on Daphnia magna, *J. Proteom.*, 2016, **137**, 45-51.

36.   D. J. Boehmler, Z. J. O'Dell, C. Chung and K. R. Riley, Bovine serum albumin enhances silver nanoparticle dissolution kinetics in a size- and concentration-dependent manner, *Langmuir*, 2020, **36**, 1053-1061.

37.   M. Long, J. Brame, F. Qin, J. Bao, Q. Li and P. J. J. Alvarez, Phosphate changes effect of humic acids on TiO_2 photocatalysis: from inhibition to mitigation of electron–hole recombination, *Environ. Sci. Technol*, 2017, **51**, 514-521.

38.   M. Drosos, M. Ren and F. H. Frimmel, The effect of NOM to TiO_2: interactions and photocatalytic behavior, *Applied Catalysis B: Environmental*, 2015, **165**, 328-334.

39.   J. Kim and K. Doudrick, Emerging investigator series: protein adsorption and transformation on catalytic and food-grade TiO_2 nanoparticles in the presence of dissolved organic carbon, *Environ. Sci. Nano*, 2019, **6**, 1688-1703.

40.   Y. Nosaka and A. Y. Nosaka, Generation and detection of reactive oxygen species in photocatalysis, *Chem. Rev.*, 2017, **117**, 11302-11336.

41.   V. G. Deepagan, D. G. You, W. Um, H. Ko, S. Kwon, K. Y. Choi, G.-R. Yi, J. Y. Lee, D. S. Lee, K. Kim, I. C. Kwon and J. H. Park, Long-circulating Au-TiO_2 nanocomposite as a sonosensitizer for ROS-mediated eradication of cancer, *Nano Lett.*, 2016, **16**, 6257-6264.

42.   Y. Liao, J. Brame, W. Que, Z. Xiu, H. Xie, Q. Li, M. Fabian and P. J. Alvarez, Photocatalytic generation of multiple ROS types using low-temperature crystallized anodic TiO_2 nanotube arrays, *J. Hazard. Mater.*, 2013, **260**, 434-441.

43.   H.-Y. Ma, L. Zhao, L.-H. Guo, H. Zhang, F.-J. Chen and W.-C. Yu, Roles of reactive oxygen species (ROS) in the photocatalytic degradation of pentachlorophenol and its main toxic intermediates by TiO_2/UV, *J. Hazard. Mater.*, 2019, **369**, 719-726.

44.   L. P. V and V. Rajagopalan, A new synergetic nanocomposite for dye degradation in dark and light, *Sci. Rep.*, 2016, **6**, 38606.

45.   J. Wang, Y. Guo, B. Liu, X. Jin, L. Liu, R. Xu, Y. Kong and B. Wang, Detection and analysis of reactive oxygen species (ROS) generated by nano-sized TiO_2 powder under ultrasonic irradiation and application in sonocatalytic degradation of organic dyes, *Ultrason. Sonochem.*, 2011, **18**, 177-183.

46.   P. Chen, L. Chen, Y. Zeng, F. Ding, X. Jiang, N. Liu, C.-T. Au and S.-F. Yin, Three-dimension hierarchical heterostructure of $CdWO_4$ microrods decorated with

Bi$_2$WO$_6$ nanoplates for high-selectivity photocatalytic benzene hydroxylation to phenol, *Applied Catalysis B: Environmental*, 2018, **234**, 311-317.

47.   Y. Ou, J.-D. Lin, H.-M. Zou and D.-W. Liao, Effects of surface modification of TiO$_2$ with ascorbic acid on photocatalytic decolorization of an azo dye reactions and mechanisms, *J. Mol. Catal. A: Chem.*, 2005, **241**, 59-64.

48.   S. Sakthivel, B. Neppolian, M. V. Shankar, B. Arabindoo, M. Palanichamy and V. Murugesan, Solar photocatalytic degradation of azo dye: comparison of photocatalytic efficiency of ZnO and TiO$_2$, *Sol. Energy Mater. Sol. Cells*, 2003, **77**, 65-82.

49.   Y. Cho and W. Choi, Visible light-induced reactions of humic acids on TiO$_2$, *Journal of Photochemistry and Photobiology A: Chemistry*, 2002, **148**, 129-135.

50.   M. Garvas, A. Testen, P. Umek, A. Gloter, T. Koklic and J. Strancar, Protein corona prevents TiO$_2$ phototoxicity, *PLoS One*, 2015, **10**, e0129577.

51.   I. Dolamic and T. Bürgi, Photocatalysis of dicarboxylic acids over TiO$_2$: an in situ ATR-IR study, *J. Catal.*, 2007, **248**, 268-276.

52.   X. Hu and T. Bürgi, In situ ATR-FTIR investigation of photodegradation of 3,4-dihydroxybenzoic acid on TiO$_2$, *Catal. Lett.*, 2016, **146**, 2215-2220.

53.   I. Dolamic and T. Bürgi, Photoassisted decomposition of malonic acid on TiO$_2$ studied by in situ attenuated total reflection infrared spectroscopy, *J. Phys. Chem. B*, 2006, **110**, 14898-14904.

54.   I. A. Mudunkotuwa and V. H. Grassian, Biological and environmental media control oxide nanoparticle surface composition: the roles of biological components (proteins and amino acids), inorganic oxyanions and humic acid, *Environ. Sci.: Nano*, 2015, **2**, 429-439.

55.   I. A. Mudunkotuwa, A. A. Minshid and V. H. Grassian, ATR-FTIR spectroscopy as a tool to probe surface adsorption on nanoparticles at the liquid-solid interface in environmentally and biologically relevant media, *Analyst*, 2014, **139**, 870-881.

56.   I. A. Mudunkotuwa and V. H. Grassian, Citric acid adsorption on TiO$_2$ nanoparticles in aqueous suspensions at acidic and circumneutral pH: surface coverage, surface speciation, and its impact on nanoparticle−nanoparticle interactions, *J. Am. Chem. Soc.*, 2010, **132**, 14986-14994.

57.   S. W. Bian, I. A. Mudunkotuwa, T. Rupasinghe and V. H. Grassian, Aggregation and dissolution of 4 nm ZnO nanoparticles in aqueous environments: influence of pH, ionic strength, size, and adsorption of humic acid, *Langmuir*, 2011, **27**, 6059-6068.

58.   I. A. Mudunkotuwa, T. Rupasinghe, C.-M. Wu and V. H. Grassian, Dissolution of ZnO nanoparticles at circumneutral pH: a study of size effects in the presence and absence of citric acid, *Langmuir*, 2012, **28**, 396-403.

59.   K. V. Abrosimova, O. V. Shulenina and S. V. Paston, FTIR study of secondary structure of bovine serum albumin and ovalbumin, *J. Phys. Conf. Ser.*, 2016, **769**, 012016.

60.   W. Chen, C. Qian, X. Liu and H. Yu, Two-dimensional correlation spectroscopic analysis on the interaction between humic acids and TiO$_2$ nanoparticles, *Environ. Sci. Technol.*, 2014, **48**, 11119-11126.

61.   K. D. Dobson and A. J. McQuillan, In situ infrared spectroscopic analysis of the adsorption of aliphatic carboxylic acids to TiO$_2$, ZrO$_2$, Al$_2$O$_3$, and Ta$_2$O$_5$ from

aqueous solutions, *Spectrochimica Acta Part A: Molecular and Biomolecular Spectroscopy*, 1999, **55**, 1395-1405.

62. K. D. Dobson and A. J. McQuillan, In situ infrared spectroscopic analysis of the adsorption of aromatic carboxylic acids to TiO_2, ZrO_2, Al_2O_3, and Ta_2O_5 from aqueous solutions, *Spectrochimica Acta Part A: Molecular and Biomolecular Spectroscopy*, 2000, **56**, 557-565.

63. A. Márquez, T. Berger, A. Feinle, N. Hüsing, M. Himly, A. Duschl and O. Diwald, Bovine serum albumin adsorption on TiO_2 colloids: the effect of particle agglomeration and surface composition, *Langmuir*, 2017, **33**, 2551-2558.

64. J. Grdadolnik and Y. Maréchal, Bovine serum albumin observed by infrared spectrometry. I. Methodology, structural investigation, and water uptake, *Biopolymers*, 2001, **62**, 40-53.

65. M. Buchholz, M. Xu, H. Noei, P. Weidler, A. Nefedov, K. Fink, Y. Wang and C. Wöll, Interaction of carboxylic acids with rutile $TiO_2(110)$: IR-investigations of terephthalic and benzoic acid adsorbed on a single crystal substrate, *Surf. Sci.*, 2016, **643**, 117-123.

66. S. A. Brandán, F. Márquez López, M. Montejo, J. J. López González and A. Ben Altabef, Theoretical and experimental vibrational spectrum study of 4-hydroxybenzoic acid as monomer and dimer, *Spectrochimica Acta Part A: Molecular and Biomolecular Spectroscopy*, 2010, **75**, 1422-1434.

67. M. Takeuchi, K. Sakamoto, G. Martra, S. Coluccia and M. Anpo, Mechanism of photoinduced superhydrophilicity on the TiO_2 photocatalyst surface, *J. Phys. Chem. B*, 2005, **109**, 15422-15428.

68. M.-h. Shao, P. Liu and R. R. Adzic, Superoxide anion is the intermediate in the oxygen reduction reaction on platinum electrodes, *J. Am. Chem. Soc.*, 2006, **128**, 7408-7409.

69. M. Hayyan, M. A. Hashim and I. M. AlNashef, Superoxide ion: generation and chemical implications, *Chem. Rev.*, 2016, **116**, 3029-3085.

70. Y. Gong, M. Zhou and L. Andrews, Spectroscopic and theoretical studies of transition metal oxides and dioxygen complexes, *Chem. Rev.*, 2009, **109**, 6765-6808.

71. Y. Gong, M. Zhou, S. X. Tian and J. Yang, Interconvertible side-on- and end-on-bonded oxo−superoxo titanium ozonide complexes, *J. Phys. Chem. A*, 2007, **111**, 6127-6130.

72. V. Diesen and M. Jonsson, Formation of H_2O_2 in TiO_2 photocatalysis of oxygenated and deoxygenated aqueous systems: a probe for photocatalytically produced hydroxyl radicals, *J. Phys. Chem. C*, 2014, **118**, 10083-10087.

73. P. A. Giguère, The infra‐red spectrum of hydrogen peroxide, *J. Chem. Phys*, 1950, **18**, 88-92.

74. T. Shibata, H. Irie, D. A. Tryk and K. Hashimoto, Effect of residual stress on the photochemical properties of TiO_2 thin films, *J. Phys. Chem. C*, 2009, **113**, 12811-12817.

75. J. Soria, J. Sanz, I. Sobrados, J. M. Coronado, A. J. Maira, M. D. Hernández-Alonso and F. Fresno, FTIR and NMR study of the adsorbed water on nanocrystalline anatase, *J. Phys. Chem. C*, 2007, **111**, 10590-10596.

76. L. K. Adams, D. Y. Lyon and P. J. J. Alvarez, Comparative eco-toxicity of nanoscale TiO_2, SiO_2, and ZnO water suspensions, *Water Res.*, 2006, **40**, 3527-3532.

77. M. Rashid, N. T. Price, M. Á. Gracia Pinilla and K. E. O'Shea, Effective removal of phosphate from aqueous solution using humic acid coated magnetite nanoparticles, *Water Res.*, 2013, **123**, 353-360.

78. N. Sakai, K. Fukuda, T. Shibata, Y. Ebina, K. Takada and T. Sasaki, Photoinduced hydrophilic conversion properties of titania nanosheets, *J. Phys. Chem. B*, 2006, **110**, 6198-6203.

79. K. Hustert and P. N. Moza, Photochemical degradation of dicarboximide fungicides in the presence of soil constituents, *Chemosphere*, 1997, **35**, 33-37.

80. S. T. Hung and M. K. S. Mak, Titanium dioxide photocatalysed degradation of organophosphate in a system simulating the natural aquatic environment, *Environ. Technol.*, 1993, **14**, 265-269.

81. P. Lei, F. Wang, S. Zhang, Y. Ding, J. Zhao and M. Yang, Conjugation-grafted-TiO_2 nanohybrid for high photocatalytic efficiency under visible light, *ACS Appl. Mater. Interfaces*, 2014, **6**, 2370-2376.

82. M. Trivedi, A. Branton, D. Trivedi, H. Shettigar, K. Bairwa and S. Jana, Fourier transform infrared and ultraviolet-visible spectroscopic characterization of biofield treated salicylic acid and sparfloxacin, *Natural Products Chemistry & Research*, 2015, **3**.

83. J. Nishijo, N. Morita, S. Asada, H. Nakae and E. Iwamoto, Interaction of theophylline with bovine serum albumin and competitive displacement by benzoic acid, *Chem. Pharm. Bull.*, 1985, **33**, 2648-2653.

84. J. Yu, J.-Y. Liu, W.-M. Xiong, X.-Y. Zhang and Y. Zheng, Binding interaction of sodium benzoate food additive with bovine serum albumin: multi-spectroscopy and molecular docking studies, *BMC Chemistry*, 2019, **13**, 95.

TOC
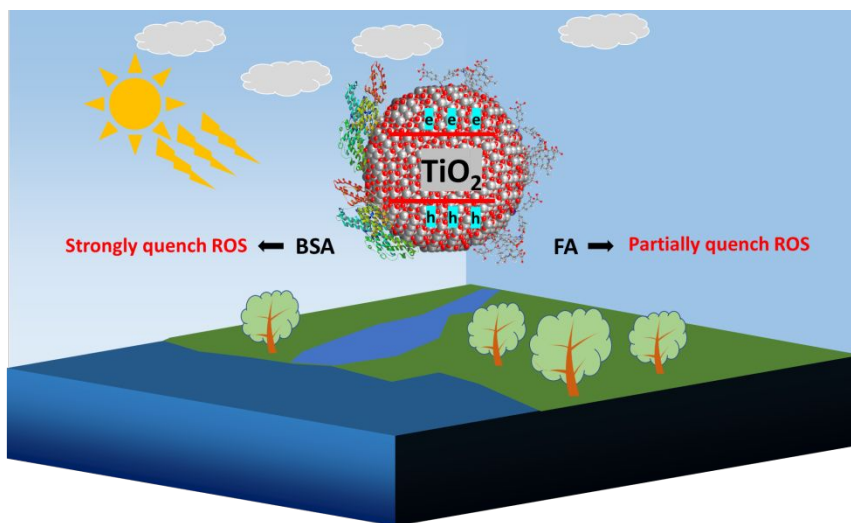
Surface coatings of biological and environmental relevance modulate the formation of reactive oxygen species upon irradiation of TiO_2 nanoparticle surfaces.